The Astrophysical Journal, 904:171 (11pp), 2020 December 1 https://doi.org/10.3847/1538-4357/abbc6f

The Secular Evolution of a Uniform Density Star Cluster Immersed in a Compressible Galactic Tidal Field

P. B. Ivanov[1] and D. N. C. Lin[2,3]
[1] Astro Space Centre of P.N. Lebedev Physical Institute, 84/32 Profsoyuznaya st., Moscow, GSP-7, 117997, Russia
[2] Department of Astronomy and Astrophysics, University of California, Santa Cruz, CA, USA
[3] Institute for Advanced Studies, Tsinghua University, Beijing 100086, People's Republic of China
Received 2020 April 23; revised 2020 September 19; accepted 2020 September 27; published 2020 December 1

Abstract

Nuclear stellar clusters are common in the center of galaxies. We consider the possibility that their progenitors assumed to be globular clusters may have formed elsewhere, migrated to, and assembled near their present location. The main challenge for this scenario is whether globular clusters can withstand the tidal field of their host galaxies. Our analysis suggests that provided the mass-density distribution of background potential is relatively shallow, as in some galaxies with relatively flat surface brightness profiles, the tidal field near the center of galaxies may be shown to be able to compress rather than disrupt a globular cluster at a distance from the center much smaller than the conventionally defined "tidal disruption radius" r_t. To do so, we adopt a previously constructed formalism and consider the secular evolution of star clusters with a homogeneous mass-density distribution. We analytically solve the secular equations in the limit that the mass density of stars in the galactic center approaches a uniform distribution. Our model indicates that a star cluster could travel to distances much smaller than r_t without disruption, thus potentially contributing to the formation of the nuclear cluster. However, appropriate numerical N-body simulations are needed to confirm our analytic findings.

Unified Astronomy Thesaurus concepts: Globular star clusters (656); Moving clusters (1076); Star clusters (1567); Stellar astronomy (1583)

1. Introduction

Gaia data reveal the prevalence of stellar streams in the Galaxy (Deason et al. 2018; Helmi et al. 2018; Koppelman et al. 2018; Myeong et al. 2018, 2019; Necib et al. 2019). Similar structures are also found in M31 (Guhathakurta et al. 2006; Gilbert et al. 2009). They are thought to be the debris of tidally disrupted stellar clusters or dwarf galaxies (Johnston et al. 1995). In the context of the ΛCDM scenario of galaxy formation, their progenitors are building blocks that converge to form larger galaxies surrounded by dark matter potential (White & Rees 1978; Blumenthal et al. 1984; Davis et al. 1985; Navarro et al. 1995, 1996, 1997). Along the course of their coalescence, loosely bound substructures are subjected to tidal disruption (Ibata et al. 1994; Oh et al. 1995; Newberg & Carlin 2016) and their debris streams contribute to the dynamical structure of the merger byproducts (Lynden-Bell & Lynden-Bell 1995). Some compact systems may withstand the tidal perturbation due to the galactic potential and be retained as globular clusters (Fall & Rees 1977). The conventional stability boundary is the "tidal disruption radius" r_t where the intruding or satellite systems' average mass density is comparable to that contributed to the galactic potential. If these systems can preserve their integrity on their way to the central regions of galactic conglomerates, they could also lead to the development of cusps versus cores (Tremaine et al. 1975; Tremaine 1976a; Dekel et al. 2003a, 2003b).

Today, there are several stellar clusters, including the Archies and Quintuplet clusters, in the vicinity of the Galactic center (Kobayashi et al. 1983; Nagata et al. 1995; Cotera et al. 1996). These clusters have much higher internal density and contain many more massive stars than all the known globular clusters in the Galaxy (Figer et al. 1999; Espinoza et al. 2009). Ideally, these clusters could have undergone orbital decay from a few kiloparsecs away to their present location within the Hubble time (Gerhard 2001). But the brief (a few megayears) lifespan of massive main-sequence stars contained in them casts a strong limit on the distance over which they may have migrated. Moreover, the intense tidal perturbation by the Galactic potential poses a challenge to their protracted sustainability (Portegies Zwart et al. 2002; Gürkan & Rasio 2005). Based on these considerations, it has been suggested that these clusters were formed close to their present-day location (Figer & Morris 2002).

Within 1 pc from the very center of the Galaxy, a nuclear cluster with $\gtrsim 10^7$ stars surrounds an $M_{\rm SMBH} \simeq 4.2 \times 10^6 M_\odot$ black hole commonly dubbed as Sgr A* (Genzel et al. 1997, 2010; Ghez et al. 1998). Although stars in the nuclear cluster are predominantly low mass and mature (Do et al. 2009), there is a population of young OB and Wolf–Rayet stars (Ghez et al. 2003). While the young stars may be formed (Goodman 2003; Levin & Beloborodov 2003; Nayakshin et al. 2007) or rejuvenated (Artymowicz et al. 1993) in situ within the past few Myr, the old star could have migrated to this confined central region if they were once members of some progenitor clusters that preserved their dynamical integrity during the course of their orbital evolution (Gerhard 2001; Madigan et al. 2014).

Many nucleated dwarf galaxies are found in the central regions of galaxy clusters (Sandage & Binggeli 1984). Nuclear clusters are also commonly found in other Milky Way–type disk galaxies (Kormendy & Ho 2013). Their contribution to the surface brightness distribution is conspicuous in their Sérsic profiles (Böker et al. 2002; Misgeld & Hilker 2011). At the

center of the more massive early-type elliptical galaxies, unresolved point sources of light are ubiquitous (Ferrarese & Ford 2005) without significant, if any, contribution from nuclear clusters. Highly variable sources that outshine their host galaxies over multiwavelength are dubbed as active galactic nuclei (AGNs). They are thought to be powered by disk accretion onto massive black holes (Lynden-Bell 1969).

The luminosity of the nuclear clusters and massive black holes can be distinguished from that of the host-galaxy background through the decomposition of the Sérsic and cusp photometric surface brightness distribution. The velocity dispersion of the host galaxies' bulge can be obtained independently with spectroscopic measurements. Despite the dichotomy between the mass and morphological classification of their host galaxies, surveys indicate that the mass M_c of both nuclear clusters and massive black holes are correlated with the velocity dispersion σ in the bulge of their host galaxies (Ferrarese & Merritt 2000; Gebhardt et al. 2000). They have similar power-law M_c–σ relationships (Ferrarese et al. 2006); albeit for intermediate-mass galaxies (such as the Milky Way) that contain both populations, the nuclear clusters are on average a few times more massive than the massive black holes (Kormendy & Ho 2013).

These tantalizing general scaling laws signal the possibility of some links between the dynamics of nuclear clusters during the evolution from relatively low mass to massive galaxies. If the merger tree is the pathway for galactic assembly, nuclear clusters and central massive black holes would coagulate together with the host building block galaxies (Pfeffer et al. 2014). After their orbits are virialized, relatively massive entities may undergo further orbital decay due to the effect of dynamical friction (Tremaine 1976b; Just et al. 2011; Neumayer et al. 2020). One important issue is under what condition can dense stellar clusters survive tidal disruption on their way to the center of galactic bulge (Fellhauer & Lin 2007; van der Marel et al. 2007).

The smallest and most common dwarf galaxies represent a microcosm of such an evolutionary pathway (Ferguson & Sandage 1991). Some dwarf galaxies contain multiple globular clusters. For example, the nearby Fornax dwarf spheroidal galaxy (dSph) hosts six globular clusters (Wang et al. 2019), and their orbital decay timescale, due to dynamical friction, has been estimated to be less than 1 Gyr (Hernandez & Gilmore 1998). These clusters remain in the field of Fornax due to the tidal stirring by the Galactic halo potential (Oh et al. 2000). In contrast, many nucleated dwarf galaxies are found inside the much larger core radius (on megaparsec scales) of some galaxy clusters (Binggeli & Cameron 1991). These nucleated dwarfs are characterized by central cusps in their surface brightness distribution. Moreover, some of these nucleated dwarfs also nest globular clusters (Miller & Lotz 2007). Their nucleated structure, including that of ultracompact dwarf galaxies (Drinkwater et al. 2003), may be byproducts of merging globular clusters (Goerdt et al. 2008). In order to account for the dichotomy between multiple floating globular clusters in the Fornax dSph and the omnipresence of nucleated dwarf galaxies in the central cores of galaxy clusters, Oh & Lin (2000) suggest that the tidal perturbation from the cluster of galaxies is compressive due to its shallow density slopes (Navarro et al. 1996). Similar processes may also play a role in the formation of the Sérsic surface brightness profile found in most elliptical galaxies (Emsellem & van de Ven 2008), heating of disk galaxies in the center of galaxy clusters (Valluri 1993), and globular clusters during their crossing of the Galactic disk (Ostriker et al. 1972).

As dwarf galaxies coalesce into larger entities, nuclear clusters on different branches of the merger tree also converge. After the postmerger virialization, the nuclear clusters' ability to undergo orbital decay and to survive against tidal disruption determine the M_c and σ values for their amalgamated byproducts. The accumulation of multiple nuclear clusters in confined regions may also promote the emergence of massive black holes (Capuzzo-Dolcetta 1993). Finally, preexisting massive black holes in the center of elliptical galaxies may maintain their local dominance by tidally disrupting incoming nuclear clusters (Gerhard 2001) at r_t comparable to or larger than the massive black holes' radius of dynamical influence (i.e., $\sim GM_{\rm SMBH}/\sigma^2$). Similarly newly arriving massive black holes may also disrupt preexisting nuclear clusters. This effect may account for the exclusion of nuclear clusters around massive black holes in the center of elliptical galaxies.

In galaxies with a highly peaked central mass concentration and a steep declining surface brightness gradient, the critical condition for tidal disruption of a globular cluster is similar to that of stars around supermassive black holes (SMBHs) or planets around stars. An entity with a mass M_0, radius R_0, an average density $\rho = 3M_0/4\pi R_0$, and a parabolic orbit undergo tidal disruption around a point mass M_G when their periastron distance between them is smaller than a few times the tidal disruption radius $r_t = (M_G/\rho)^{1/3}$ or, equivalently, when the "average density" associated with the point-mass potential $\rho_G = 3M_G/4\pi r_t^3$ is $\gtrsim\rho$ (Frank & Rees 1976). A similar tidal limiting radius also applies to self-gravitating entities on a circular orbit (Chandrasekhar 1969). But around the central regions of some galaxies where the density is a weakly declining function of distance from them, this condition is modified by the additional gravity from the background stars in the concentric shells that sandwich the satellite system. Qualitatively, around a homogeneous background, stars farther away from the center of the bulge accelerate more rapidly than those closer to the center. This effect leads to a tidal compression (Oh & Lin 2000; Masi 2007).

In this paper, we provide a quantitative analysis to verify the possibility that a compressive rather than a disruptive tidal field could preserve the integrity of globular clusters orbiting around a spherically symmetric distribution of mass at distances much smaller than r_t. In Section 2, we consider an idealized analytic model to examine the condition for tidal stability of a stellar cluster following the work of Mitchell & Heggie (2007), which itself is based on the model of so-called Freeman (1966a, 1966b, 1966c) bar. This model has the advantage that the cluster immersed in a stationary tidal field maintains a uniform distribution of its mass density, ρ, and has the shape of a general ellipsoid with unequal semimajor axes. This approach greatly simplifies analytic analysis of the model. Then, we formulate equations describing secular evolution of the model proceeding when its orbit that is assumed to be circular shrinks as a result of dynamical friction. In Section 3, we discuss solutions to the secular equations. These solutions describe the adiabatic adjustment in the phase-space distribution subjected to changes in the external tidal fields. At first, we consider the strong tidal limit and determine the critical tidal disruption condition for power-law density distribution for the background galaxy, $\rho_G \propto R^{-k}$, under the assumption that the

density in the galactic background decreases with radius gradually, and accordingly, k is small. We show that in this case, as expected in the bulge of some galaxies, these clusters are practically indestructible by the tidal perturbation of the background galaxy. Later in this section we show that the cluster in our model remains spherically symmetric in the formal limit $k = 0$ corresponding to the homogeneous density distribution for any strength of tidal field and that its radius, a, is described by a solution to a quartic equation. We take into account a nonzero, but formally small, value of k in the framework of a perturbation theory and show how the critical semimajor axes of the cluster as well as its density depend on the strength of the tidal field. We note that clusters with a centrally concentrated density profile are more likely to survive tidal disruption than the homogeneous model we have adopted. Therefore, our criteria for clusters' preservation in a relatively shallow background potential are robust. We explore some astrophysical applications based on the King model, several commonly used parameterized models, the empirical Sérsic model for galactic bulges and elliptical galaxies, and a composite model for the Milky Way galaxy in Section 4. We summarize our results and discuss their limitations and implication in Section 5. Additionally, in Section 5 we provide a qualitative argument, which allows us to suggest that at least some more realistic models of star cluster evolution in a tidal field of a galaxy corresponding to nearly homogeneous mass density of galactic matter could behave similarly to our idealized toy model.

2. An Analytic Model of a Star Cluster in a Compressive Tidal Field

For mathematical convenience, we adopt the boundary conditions that (1) the density of the background galaxy is spherically symmetric, (2) the cluster is on a circular orbit around the center of the galaxy, and (3) the mass density inside the cluster is homogeneous. Under these conditions, we consider (1) the gravitation potential in terms of a triaxial ellipsoid (Section 2.1), (2) the solutions of the equation of motion for stars in the frame that is comoving with the cluster and corotating with its orbital frequency (Section 2.2), and (3) normal modes, frequencies of stellar motion, and adiabatic invariants in terms of action variables associated with the normal modes. These quantities enable us to extrapolate the density and shape adjustments to gradually increase in the tidal potential (Section 2.3). Physically, this approximation represents the slow decay of the cluster's nearly circular orbit to the proximity of the galactic center, starting from very large galactic distances where the external field is negligible and the stellar cluster is spherical symmetric.

2.1. Basic Definitions and Relations

We adopt the same noninertial right-handed Cartesian coordinate system as in Bertin & Varri (2008) with x-, y-, and z-axes directed outward from galactic center, in the orbital plane, and perpendicular to it, respectively. In this system equations of motion of stars take the form

$$\ddot{x} - 2\Omega\dot{y} + \frac{\partial\Phi}{\partial x} - \gamma^2 x = 0, \quad \ddot{y} + 2\Omega\dot{x} + \frac{\partial\Phi}{\partial y} = 0,$$
$$\ddot{z} + \frac{\partial\Phi}{\partial z} + \Omega^2 z = 0, \tag{1}$$

where the dot stands for the time derivative, Ω is the angular frequency of orbital motion assumed to be circular:

$$\Omega^2 = \frac{1}{R}\frac{\partial}{\partial R}\Phi_G, \tag{2}$$

R is the distance from galactic center, and Φ_G is the gravitational potential of a galaxy. The quantity γ can be expressed in terms of Ω and epicyclic frequency, κ, as $\gamma^2 = 4\Omega^2 - \kappa^2 = \frac{1}{R}\frac{d}{dR}\Phi_G - \frac{d^2}{dR^2}\Phi_G$. For a spherically symmetric distribution of galactic mass density, ρ_G, assumed from now on we can express Ω and γ in terms of ρ_G as

$$\Omega^2 = \frac{4\pi G}{R^3}\int R^2 dR\rho_G, \quad \gamma^2 = -\frac{4\pi G}{R^3}\int R^3 dR\frac{d}{dR}\rho_G, \tag{3}$$

where G is the gravitational constant. Note that the latter equation yields $\gamma^2 > 0$.

Physically, the sign of γ^2 is determined by interplay between tidal and centrifugal forces acting in the x direction, relative to the cluster center. Although it is easy to show that the tidal force is attractive, when $\gamma^2 < \Omega^2$ the centrifugal is always repulsive with its absolute value always larger than that of tidal force. Thus, the combination of two forces is always repulsive when $\gamma^2 > 0$, and neutral when $\gamma^2 = 0$, which corresponds to a homogeneous density of galactic stars.

The gravitational potential of stars in the cluster Φ obeys the Poisson equation

$$\Delta\Phi = 4\pi G\rho, \tag{4}$$

where Δ is the Laplace operator and ρ is the mass density of the stars.

Equations (1) have the well-known Jacobi integral

$$E = \frac{v^2}{2} + \Phi_{ext} + \Phi, \tag{5}$$

where v is the absolute value of velocity of a star and

$$\Phi_{ext} = \frac{\Omega^2 z^2}{2} - \frac{\gamma^2 x^2}{2} \tag{6}$$

is the sum of potentials of tidal and centrifugal forces.

2.2. Equations of Motion in Canonical Form for a Model with Homogeneous Density Distribution

In what follows we are going to use a model of a star cluster proposed in Mitchell & Heggie (2007), which is related to the Freeman (1966a, 1966b, 1966c) models for uniform density rotating bars. Although the model is rather artificial it has the advantage that the stellar density of the cluster is homogeneous and the cluster has the form of an ellipsoid. This allows for an analytic treatment of the problem on hand.

We use below the fact that the gravitational potential of an ellipsoid having a uniform density ρ has the quadratic form

$$\Phi = \pi G\rho\sum_{i=1,3} A_i x_i^2, \tag{7}$$

where we set to zero the unimportant constant part and the indices 1, 2, and 3 stand for x, y, and z, respectively. The dimensionless quantities A_i can be expressed in terms of two angles, θ and ϕ, determined by ratios of a_i. Namely, let us arrange the axes a_i in ascending order $a_{\min} \leqslant a_{\rm int} \leqslant a_{\max}$ and introduce θ and ϕ according to the relations $\sin\theta = \sqrt{\frac{a_{\max}^2 - a_{\rm int}^2}{a_{\max}^2 - a_{\min}^2}}$

and $\cos\phi = \frac{a_{\min}}{a_{\max}}$. It may be then shown that A_i can be expressed in terms of incomplete elliptic integrals; see, e.g., Chandrasekhar (1969). For our purposes, however, it is more convenient to use the equivalent explicit expressions

$$A_1 = \frac{2\cos\phi\Delta^{1/2}(\theta,\,\phi)}{\sin^3\phi}\int_0^{\phi} d\phi' \frac{\sin^2\phi'}{\Delta^{1/2}(\theta,\,\phi')}, \tag{8}$$

$$A_2 = \frac{2\cos\phi\Delta^{1/2}(\theta,\,\phi)}{\sin^3\phi}\int_0^{\phi} d\phi' \frac{\sin^2\phi'}{\Delta^{3/2}(\theta,\,\phi')}, \tag{9}$$

where $\Delta(\theta,\,\phi) = 1 - \sin^2\theta\,\sin^2\phi$, and we take into account that $\sum_{i=1}^{i=3} A_i = 2$, and therefore $A_3 = 2 - (A_1 + A_2)$.

Using the expression (7) Equation (1) can be brought in a standard form by introducing three new frequencies:

$$\omega_1^2 = 2\pi G\rho A_1 - \gamma^2,\;\; \omega_2^2 = 2\pi G\rho A_2,\;\; \omega_3^2 = 2\pi G\rho A_3 + \Omega^2. \tag{10}$$

We have

$$\ddot{x} - 2\Omega\dot{y} + \omega_1^2 x = 0,\;\; \ddot{y} + 2\Omega\dot{x} + \omega_2^2 y = 0,\;\; \ddot{z} + \omega_3^2 z = 0. \tag{11}$$

It is seen that motion in the vertical direction corresponds to a simple oscillator having the energy $E_3 = \frac{1}{2}(\dot{z}^2 + \omega_3^2 z^2)$. It is well known that the so-called action variable

$$I_3 = E_3/\omega_3 \tag{12}$$

is an adiabatic invariant, which stays constant when parameters of the problem change slowly.

The "horizontal" coordinates x and y are coupled by Coriolis force. Accordingly, motion in the horizontal direction corresponds to a two-dimensional rotating oscillator. In order to introduce the action variables I_1 and I_2 for such an oscillator we are going to introduce a canonical change of variables bringing the systems to the form of two decoupled linear oscillators.

For that, at first we integrate the first two Equations of (11) representing the general solution in the following form:

$$x = \alpha_1\tilde{x}_1 + \tilde{x}_2, \quad y = \tilde{y}_1 + \alpha_2\tilde{y}_2, \tag{13}$$

where

$$\tilde{x}_{1,2} = D_{1,2}\cos\Psi_{1,2} \quad \tilde{y}_{1,2} = D_{1,2}\sin\Psi_{1,2}, \tag{14}$$

$\Psi_{1,2} = \sigma_{1,2}t + \Psi_{1,2}^0$, D_i and Ψ_i^0 are arbitrary constants, while eigenfrequencies σ_i can be found as solutions of a biquadratic equation

$$\sigma_{1,2}^2 = \frac{1}{2}(\omega_1^2 + \omega_2^2 + 4\Omega^2 \pm \sqrt{(\omega_1^2 + \omega_2^2 + 4\Omega^2)^2 - 4\omega_1^2\omega_2^2}), \tag{15}$$

and

$$\alpha_i = \frac{2\Omega\sigma_i}{\omega_i^2 - \sigma_i^2}, \tag{16}$$

where the indices $i = 1, 2$.

It is convenient to represent equations of motion in the horizontal direction in the canonical form introducing the corresponding Hamiltonian

$$H = \frac{(P_1 + \Omega y)^2}{2} + \frac{(P_2 - \Omega x)^2}{2} + \frac{1}{2}(\omega_1^2 x^2 + \omega_2^2 y^2), \tag{17}$$

where P_1 and P_2 are canonical conjugates of x and y, respectively.

Now one can prove by a direct substitution that when new coordinates, $\hat{q}_i$, and momenta, $\hat{P}_i$, are introduced according to the rule

$$\tilde{y}_1 = \frac{1}{f_1^{1/2}}\hat{P}_1,\;\; \tilde{x}_1 = -\frac{\sigma_1}{f_1^{1/2}}\hat{q}_1,\;\; \tilde{x}_2 = \frac{1}{f_2^{1/2}}\hat{P}_2\;\; \tilde{y}_2 = \frac{\sigma_2}{f_2^{1/2}}\hat{q}_2, \tag{18}$$

where

$$f_i = \frac{\sigma_i^2(\sigma_i^2 - \sigma_j^2)}{(\sigma_i^2 - \omega_i^2)}, \tag{19}$$

where $i \neq j$, the coordinate transformation (13) and (18) together with corresponding transformation of the momenta

$$P_1 = -(\alpha_1\sigma_1 + \Omega)\tilde{y}_1 - (\sigma_2 + \alpha_2\Omega)\tilde{y}_2, \tag{20}$$

$$P_2 = (\sigma_1 + \alpha_1\Omega)\tilde{x}_1 + (\Omega + \alpha_2\sigma_2)\tilde{x}_2 \tag{21}$$

provide a canonical transformation, which brings Hamiltonian (17) to the diagonal form

$$H = E_1 + E_2, \quad E_i = \frac{1}{2}(\hat{P}_i^2 + \sigma_i^2\hat{q}_i^2) = \frac{1}{2}f_i D_i^2. \tag{22}$$

Accordingly, the quantities

$$I_i = \frac{E_i}{\sigma_i} = \frac{1}{2\sigma_i}f_i D_i^2 \tag{23}$$

are the action variables. Therefore, they are adiabatic invariants.

2.3. Equations for Secular Evolution of a Star Cluster with a Homogeneous Stellar Density

Following Mitchell & Heggie (2007), we use the simple expressions for the gravitational potential discussed above. It is assumed that, initially, at a moment of time $t = t_0$, the cluster is situated far from galactic center and the tidal effects as well as the ones due to the presence of Coriolis force can be neglected. Also, we assume that initially the cluster has the form of a sphere of radius r_0 and mass M, and its initial density is $\rho_0 = \frac{3M}{4\pi r_0^3}$. Therefore, at $t = t_0$ we can set in Equations (10) $\Omega = \gamma = 0$. Due to the assumption of spherical symmetry $A_1 = A_2 = A_3$, it is easy to see from (10) that $\omega_1(t_0) = \omega_2(t_0) = \omega_3(t_0) \equiv \omega_0$, where

$$\omega_0 = \sqrt{\frac{4\pi}{3}G\rho_0}. \tag{24}$$

This quantity is used as a normalization factor in Section 3.1.

The orbit of the cluster assumed to be circular shrinks with time and, therefore, at later times the tidal and Coriolis effects should be taken into account. The frequencies (10) are, in general, different from each other; the main axes of ellipsoid, a_1, a_2, and a_3 are different from r_0; and the stellar density ρ differs from ρ_0.

It is the purpose of this section to find equations for the evolution of the main axes and density under the assumption of the slowness of change of the cluster orbit provided that initially their values are equal to r_0 and ρ_0, respectively. We consider the so-called β-model of Mitchell & Heggie (2007) where the amplitude D_2 defined in (14) is equal to zero for all stars retained by the cluster. Additionally, it was shown in

Mitchell & Heggie (2007) that, for self-consistency, the relation

$$|\alpha_1| = \frac{a_1}{a_2}, \tag{25}$$

where α_1 is defined in (16), should be satisfied for all times. This relation stems from the following arguments. The solution to Equation (11) describing vertical motion of a star can be written in the form $z = D_3 \cos\Psi_3$, where $\Psi_3 = \omega_3 t + \Psi_3^0$, D_3, and Ψ_3^0 are constants of motion. Obviously, a star attains the maximal value of $z = D_3$ when $\cos\Psi_3 = 1$. At these moments of time the orbit must touch the boundary of the ellipsoid, and accordingly, there should be $\frac{x^2}{a_1^2} + \frac{y^2}{a_2^2} + \frac{z^2}{a_3^2} = 1$. From (13) and (14) it follows that this condition can be rewritten in the form

$$\frac{\alpha_1^2 D_1^2 \cos^2\Psi_1}{a_1^2} + \frac{D_1^2 \sin^2\Psi_1}{a_2^2} + \frac{D_3^2}{a_3^2} = 1. \tag{26}$$

Equation (26) must be satisfied for all values of Ψ_1, which is possible only when Equation (25) is valid. In this case from (26) it follows that

$$\frac{D_1^2}{a_2^2} + \frac{D_3^2}{a_3^2} = 1. \tag{27}$$

From Equation (27) it is seen that the maximal value of D_1 is a_2 and the maximal value of D_3 is a_3.

Now we express the adiabatic invariants I_3 and I_1 given by Equations (12) and (15) through a_2 and a_3 assuming that the former invariant is evaluated for a trajectory with the maximal D_3 and $D_1 = 0$, while the latter one is evaluated for a trajectory with the maximal D_1 and $D_3 = 0$. Since these quantities stay approximately constant during the evolution of our system they can be evaluated twice, for the initial moment of time and for some arbitrary time, thus linking values of the quantities of interest to the initial ones. We have

$$a_1 = \sqrt{\frac{2\omega_0\sigma_1\alpha_1^2}{f_1}}\, r_0, \quad a_2 = \sqrt{\frac{2\omega_0\sigma_1}{f_1}}\, r_0, \quad a_3 = \sqrt{\frac{\omega_0}{\omega_3}}\, r_0. \tag{28}$$

Note the factor 2 in the first and second expressions in (28). It appears because $f_1 \to 2\omega_0$ in the limit $\Omega \to 0$; see Equation (45).

Additionally, from the law of mass conservation we obtain the obvious relation

$$\rho = \frac{\rho_0 r_0^3}{a_1 a_2 a_3}. \tag{29}$$

Equations (28) and (29) are the evolution equations of our model. In general, they must be solved numerically, since values of main axes enter the right-hand side implicitly, through the dependency of the coefficients A_1, A_2, and A_3 on them. Note that the solutions should be different from the solutions of an analogous incompressible model. This difference stems from the fact that the analog of pressure, velocity tensor $\langle v_i v_j \rangle$, where brackets stand for averaging with a distribution function in phase space, is not zero at the surface in the stellar dynamical model.

3. Solutions of the Secular Equations

Based on the above formalism, we examine the condition under which the tidal perturbation from the galactic potential is compressive. Around a point-mass potential, a cluster would be tidally disrupted if its galactic orbital frequency ω is larger than its characteristic internal frequency ω_0. However, around a galaxy with a shallow density distribution, a cluster may preserve its integrity deep in the galactic potential where $\omega \gg \omega_0$. We first consider an idealized case of negligible γ^2 that corresponds to a homogeneous density distribution of galactic stars. We show that the compression by the galactic tide preserves the spherical shape of the cluster. When the first-order contribution of a small γ^2 is taken into account, we identify the condition for tidal disruption in terms of the ratio between γ^2 and angular frequency Ω^2 (Section 3.2). We introduce a idealized power-law density for the galaxy and estimate the critical radius r_t outside which a cluster would withstand tidal disruption (Section 3.3). In the limit of small γ^2, we show that the tidal perturbation from a background potential due to a relatively flat density distribution is predominantly compressive (Section 3.4). For the Milky Way, we suggest the disk contribution to the tidal field, if dominant, can ensure the survival of migratory stellar cluster (Section 4.3).

3.1. Natural Units

In what follows it it convenient to express all quantities of the dimension of a frequency entering the problem apart from γ, such as σ_i, ω_i, and Ω in units of ω_0; semimajor axes a_i in units of r_0; and density in units of ρ_0. This will be implicitly implied hereafter.

We also introduce the ratio of γ to angular frequencies of the cluster's orbit around the galaxy,

$$\tilde{\gamma} \equiv \gamma/\Omega. \tag{30}$$

For a point-mass galactic potential, it is $\sqrt{3}$. But we are considering potentials for galaxies with relatively shallow density distribution. In this case, $\tilde{\gamma}$ can be treated as a small parameter, and a simple analytic solution of the secular equations is possible.

3.2. The Limit of a Strongly Compressed Star Cluster

First, let us consider a star cluster situated deep within the potential well of a galaxy assuming that $\Omega \gg 1$. Note that the condition $\Omega > 1$ may be used as the tidal disruption condition in the standard situation when $\tilde{\gamma} \sim 1$. We assume, however, that $\tilde{\gamma}$ is small and may be neglected in the leading approximation. In this limit Equation (15) tells us that $\sigma_1 \approx 2\Omega$ and $\sigma_2 \approx 0$. In this case it is seen from Equations (16) and (19) that we have $\alpha_1 \approx -1$ and $f_1 \approx 4\Omega^2$. Using Equation (25) we find that $a_1 \approx a_2$, while Equations (28) tell us that $a_1 \approx a_2 \approx a_3 \approx \frac{1}{\sqrt{\Omega}}$. In summary, in the leading approximation a strongly compressed star cluster maintains its spherical form with both ϕ and θ being small and

$$a \equiv a_i \approx \Omega^{-1/2}, \quad \rho \approx \Omega^{3/2}. \tag{31}$$

The next-order corrections taking into account effects of nonzero $\tilde{\gamma}$ and self-gravity can be easily found using the fact that, for a spherical cluster, all A_i in Equation (10) are equal to $2/3$, and that we can can use these and the expressions (31) when considering ω_i in Equation (15), since these characteristic

frequencies are assumed to be much smaller than Ω. We obtain from (10) $\sigma_1 \approx 2\Omega\left(1 + \frac{{\omega_1}^2 + {\omega_2}^2}{8}\right)$. Equations (25) and (28) can be used again to find the corrected values of a_i and ρ. Since calculations are straightforward we show only the following results:

$$a_1 = \frac{1}{\Omega^{1/2}}\left(1 - \frac{1}{4\Omega^{1/2}} + \frac{\tilde{\gamma}^2}{16}\right), \tag{32}$$

$$a_2 = \frac{1}{\Omega^{1/2}}\left(1 - \frac{1}{4\Omega^{1/2}} + \frac{3\tilde{\gamma}^2}{16}\right), \tag{33}$$

$$a_3 = \frac{1}{\Omega^{1/2}}\left(1 - \frac{1}{4\Omega^{1/2}}\right), \tag{34}$$

$$\rho \approx \Omega^{3/2}\left(1 + \frac{3}{4\Omega^{1/2}} - \frac{\tilde{\gamma}^2}{4}\right). \tag{35}$$

From the above equations, it is seen that the corrections are small when $\tilde{\gamma} < 1$ and $\Omega \gg 1$, and that $a_1 < a_2$, i.e., the cluster elongation in the direction of motion is larger than the one in the direction of the galactic center. This orientation is orthogonal to that of the analogous incompressible fluid model, where the axis is elongated in the direction of the galactic center.

Although the corrections get smaller with an increase of Ω when it gets sufficiently large ω_1 defined in Equation (10) becomes imaginary, which results in runaway of stars from the cluster and its disruption. Equating ω_1 to zero and using $A_1 = 2/3$ and the expressions (31) we find a very simple criterion of tidal disruption of a cluster in our model—the cluster is disrupted when

$$\tilde{\gamma} \equiv \gamma/\Omega > \Omega^{-1/4}. \tag{36}$$

3.3. A Simple Model of Galactic Tidal Field

As an example of distribution of galactic density let us consider a power-law dependence

$$\rho_G = \rho_0 (R/R_0)^{-k}, \tag{37}$$

noting that it is normally expected that a cluster would be disrupted at $R \sim R_0$. From Equation (3) it follows that in case of distribution (37) we have

$$\tilde{\gamma} = k^{1/2}, \quad \Omega = \left(\frac{3}{3-k}\right)^{1/2} \tilde{R}^{-k/2}, \tag{38}$$

where $\tilde{R} = R/R_0$. From our criterion for tidal disruption (36) it follows that the cluster is disrupted when $R < R_T$, where

$$R_T = \left(\frac{3}{3-k}\right)^{1/k} k^{4/k} R_0. \tag{39}$$

It is very interesting to note that according to the criterion (39) the cluster is practically indestructible even when k is not very small (see Figure 1). Say, when $k = 0.5$ we have $R_T \approx 6 \times 10^{-3} R_0$.

3.4. An Analytic Solution of the Secular Equations in the Limit of Small $\tilde{\gamma}$

Equation (35) tells that when the $\tilde{\gamma} = 0$ cluster remains spherical in the limit of strong compression $\Omega \gg 1$. On the other hand, it is obviously spherical when the tidal field is absent and $\Omega = 0$. This suggests that it is reasonable to assume that it is spherical when $\gamma = 0$ for any value of Ω. We are going to show that this is indeed the case and consider the following ansatz for the axis a_i and the frequencies ω_i:

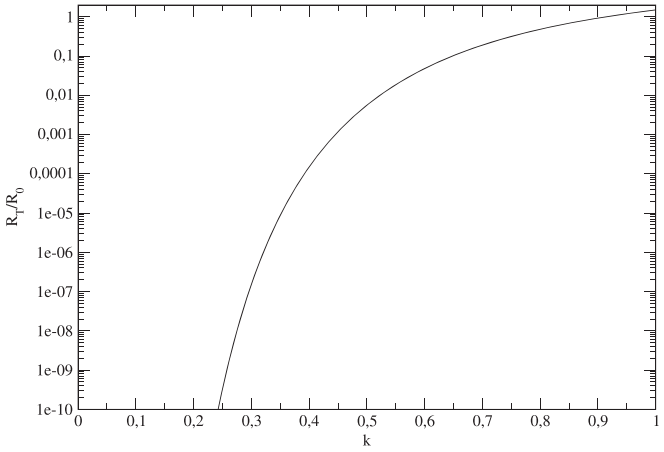

Figure 1. The dependence of R_t on k given by Equation (39).

$$a_i = a_0(1 - \delta_i), \quad \omega_{1,2}^2 = a_0^{-3} + \Delta_{1,2},$$
$$\omega_3^2 = a_0^{-3} + \Delta_3 + \Omega^2, \tag{40}$$

where it is implied that both δ_i and Δ_i are small being proportional to $\tilde{\gamma}^2$. Substituting the expressions for the frequencies into (10) and (69) and taking into account (29) we get

$$\Delta_1 = \frac{3}{5a_0^3}(\delta_2 + \delta_2 + 3\delta_1) - \gamma^2,$$
$$\Delta_{2,3} = \frac{3}{5a_0^3}(\delta_{1,2} + \delta_{3,1} + 3\delta_{2,3}). \tag{41}$$

Now we substitute (41) in (15) to obtain

$$\sigma_{1,2}^2 = (\omega_* \pm \Omega)^2\left(1 + \frac{\Delta_1 + \Delta_2}{4\omega_*(\omega_* \pm \Omega)}\right), \tag{42}$$

where

$$\omega_* = \sqrt{\Omega^2 + a_0^{-3}}. \tag{43}$$

Note that when $\tilde{\gamma} = 0$ $\omega_* = \omega_3$.

We substitute (41) in (16) and (19). From (16) we get

$$\alpha_1^2 = 1 + \frac{\Delta_1 - \Delta_2}{2\Omega(\omega_* + \Omega)}, \tag{44}$$

and from (19) we get

$$\frac{2\sigma_1}{f_1} = \frac{1}{\omega_*}\left(1 + \frac{\Delta_2 - \Delta_1}{4\Omega(\omega_* + \Omega)} - \frac{\Delta_1 + \Delta_2}{4\omega_*^2}\right). \tag{45}$$

Note that in the limit $\Omega \to 0$ we have $\sigma_1, \omega_* \to \omega_0$ and, therefore, $f_1 \to 2\omega_0$. This explains the factor 2 in (28). From the expression for ω_3 and the definition of Δ_3 we get $\omega_3 = \omega_*(1 + \frac{\Delta_3}{2\omega_*^2})$.

Now we substitute the expressions above into the secular Equation (28). All Equations (28) result in only one zero-order

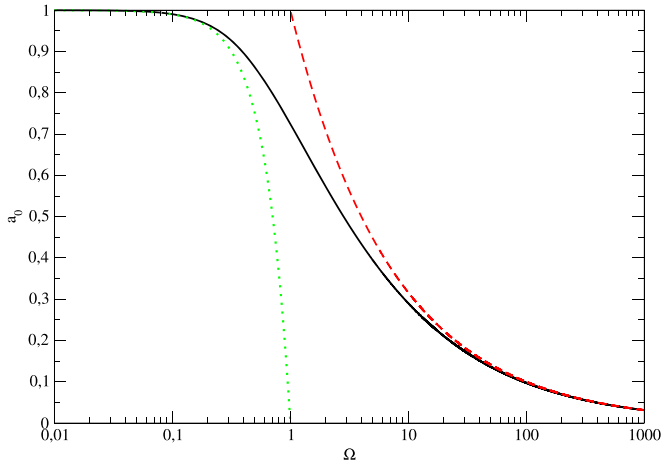

Figure 2. The result of the solution of Equation (46) together with the corresponding approximate expressions. See the text for a description of the different curves.

equation for the quantity a_0

$$a_0^2 = \frac{1}{\omega_*} = \frac{1}{\sqrt{\Omega^2 + a_0^{-3}}}. \tag{46}$$

This justifies our assumption that when $\tilde{\gamma} = 0$ the cluster remains spherical for all values of Ω. It is obvious that (46) results in a quartic equation for a_0 with coefficients depending only on Ω. The physically acceptable solution of this equation is shown in Figure 2 as a solid line. As a dashed line we show the corresponding asymptotic solution in the limit of large Ω, $a_0 \approx \Omega^{-1/2}$, and as a dotted line the approximate solution in the limit of small Ω, $a_0 \approx 1 - \Omega^2$, is shown.

The perturbed part of the secular equations can be compactly written introducing new variables $\delta_\pm = \delta_1 \pm \delta_2$ and $\Delta_\pm = \Delta_1 \pm \Delta_2$. We have

$$\delta_{3,+} = \frac{\Delta_{3,+}}{4\omega_*^2}, \quad \delta_- = \frac{\Delta_-}{4\Omega(\omega_* + \Omega)}. \tag{47}$$

We substitute (41) into (47) to obtain

$$\delta_- = \frac{\delta_*}{\Omega^2 a_0^4 + \Omega a_0^2 + \frac{3}{10} a_0}, \quad \delta_+ = -\frac{\left(1 + \frac{9}{10} a_0\right)\delta_*}{1 - \frac{21}{20} a_0 + \frac{9}{40} a_0^2}, \tag{48}$$

$$\delta_3 = -\frac{3\delta_*}{20\left(1 - \frac{21}{20} a_0 + \frac{9}{40} a_0^2\right)}, \quad \text{where} \quad \delta_* = \frac{\tilde{\gamma}^2 \Omega^2}{4\omega_*^2}. \tag{49}$$

The original quantities can be easily recovered from the obvious relations $\delta_{1,2} = \frac{1}{2}(\delta_+ \pm \delta_-)$. When considering the limit $\Omega \to \infty$ it is possible to show that the expressions (48) and (49) give corrections proportional to $\tilde{\gamma}^2$, which are in agreement with the previous result (35).

It is seen from (46), (48), and (49) that the ratios $\delta_i/\tilde{\gamma}^2$ are functions of Ω only. We represent them in Figure 3 for δ_1, δ_2, and δ_3 shown as solid, dashed, and dotted lines, respectively. One can see from this figure that all δ_i are negative. Thus, the presence of a nonzero, but small γ always leads to a small expansion of the cluster as expected. It is also seen that the absolute value of δ_3 is larger than that of δ_2 when $\Omega \leqslant \Omega_* \approx 0.46$. When $\Omega \to \infty$ $\delta_3 \to 0$.

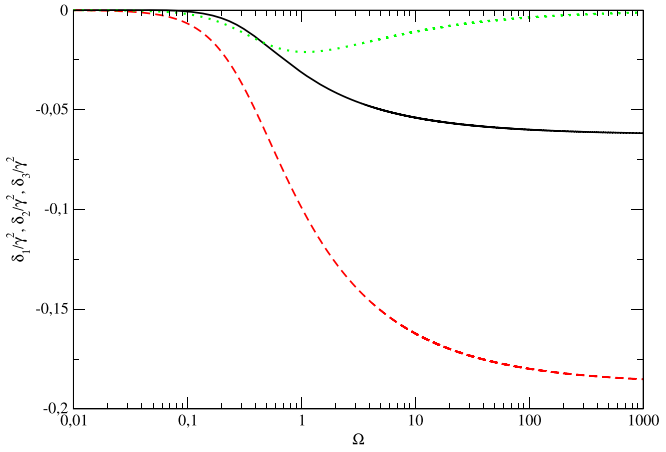

Figure 3. We show solutions (48) and (49) of Equation (47). See the text for a description of different curves.

4. Applications to Some Empirical Galaxy Models

4.1. Parametric Model Potentials

In the analysis of observational data for the central regions of galaxies, a frequently used prescription is the modified Hubble profile (Côté et al. 2006) in which the density at $R < 2R_K$ can be approximated as

$$\rho_G = \rho_K(R) \simeq \frac{\rho_c}{(1 + R^2/R_K^2)^{3/2}}, \tag{50}$$

where $R_K = \sqrt{9\sigma^2/4\pi G\rho_c}$ is the King radius and ρ_c and σ are the central density and velocity dispersion (Binney & Tremaine 2008). Since ρ_K is approximately homogeneous and $k \sim 0$, the tidal perturbation in compressive. But in the outer regions of the King model, $\rho_K(R) \propto R^{-3}$ and the tidal perturbation is disruptive.

For the bulge of disk galaxies and elliptical galaxies, the classical Jaffe (1983) potential is generated from a density distribution

$$\rho_G = \rho_J(R) = \frac{\rho_B}{(R/R_B)^2[1 + (R/R_B)^2]}, \tag{51}$$

where ρ_B is a normalized density and R_B is the scaling parameter. For $R \ll R_B$ $\rho_J(R) \propto R^{-2}$ and $k = 2$ the tidal perturbation is disruptive.

Another frequently used Hernquist (1990) potential is generated from a density distribution

$$\rho_G = \rho_H(R) = \frac{\rho_{H0}}{(R/R_H)[1 + (R/R_H)]^3}, \tag{52}$$

where ρ_{H0} is a normalized density and R_H is the scaling parameter. For $R \ll R_H$ $\rho_H(R) \propto R^{-1}$ and $k = 1$ the tidal perturbation is disruptive.

A more general η potential (Tremaine et al. 1994) arising from the associated density distribution is determined by

$$\rho_G = \rho_\eta(R) = \frac{\eta\rho_{\eta 0}}{(R/R_\eta)^{3-\eta}[1 + (R/R_\eta)]^{1+\eta}}, \quad 0 < \eta \leqslant 3, \tag{53}$$

where $\rho_{\eta 0}$ is a normalized density, R_η is the scaling parameter, and η is a power index parameter. For $R \ll R_\eta$, $\rho_\eta(R) \propto R^{\eta-3}$ and $k = \eta - 3$ such that it is reduces to the King, Herquist, and

Jaffe model with $\eta = 3$, 2, and 1, respectively. Moreover, contribution from the point-mass potential of the SMBH can be added to the η potential. Depending on the value of η, the tidal perturbation can be both compressive and disruptive.

4.2. Empirical Sérsic Models

The surface brightness I of elliptical galaxies and the bulge of spiral galaxies is commonly modeled (Kormendy et al. 2009) in terms of an empirical Sersic (1968) profile with $I = I(0)\exp[-b_n(D/R_S)^{1/n}]$, where $I(0)$ is central surface brightness, D is the projected distance from the center, R_S is the scaling radius, $b_n = 2n - 0.324$, and $1 \leqslant n \leqslant 15$ is the fitting power index. For a spheroid, the associated density at a distance r from the galactic center can be approximated (Prugniel & Simien 1997; Terzić & Graham 2005) by

$$\rho_G = \rho_S(R) = \rho_{S0}(R/R_S)^{-p_n}\exp[-b_n(R/R_S)^{1/n}], \quad (54)$$

where ρ_{S0} is a normalization constant. The power index can be approximated as $p_n = 1 - 0.6097/n + 0.05563/n^2$ for $0.6 \leqslant n \leqslant 10$ and $10^{-2} \leqslant R/R_S \leqslant 10^3$. Observational fits (Graham & Driver 2005) show that the magnitude of n increases from 0.5 to 10 for a galaxy mass in the range of 10^7–$10^{12}M_\odot$. At the low-mass end $k \sim 0$ and the tidal perturbation is compressive, whereas for the massive elliptical galaxies (with n approaching 10), $\rho_S(R) \propto R^{-1}$ near the center so that the tidal perturbation is disruptive. We thank an anonymous referee for noting to us that the trend of the Sérsic index most likely applies to the outer slopes, not the inner regions, and more massive galaxies may have cores with lower central densities. This correlation may account for the dichotomy between the presence of nuclear clusters around galaxies with comparable or less mass than the Galaxy and their absence in massive elliptical galaxies.

4.3. Galactic Potential

There are several empirical prescriptions for the gravitational potential of the Galaxy. In general, contribution to Φ_G is considered to be the sum of that due to the central SMBH ($\Phi_{\rm SMBH}$), the Galactic bulge ($\Phi_{\rm BULGE}$), the Galactic disk ($\Phi_{\rm DISK}$), and the halo ($\Phi_{\rm HALO}$) (Gnedin et al. 2005; Widrow & Dubinski 2005), where

$$\Phi_G = \Phi_{\rm SMBH} + \Phi_{\rm bulge} + \Phi_{\rm disk} + \Phi_{\rm halo}, \quad (55)$$

$$\Phi_{\rm SMBH} = -GM_{\rm SMBH}/R, \quad (56)$$

$$\Phi_{\rm bulge} = -GM_{\rm bulge}/(R + R_{\rm bulge}), \quad (57)$$

$$\Phi_{\rm disk} = -GM_{\rm disk}\Big/[(\sqrt{(z^2 + b^2)} + a)^2 + \varpi^2]^{1/2}, \quad (58)$$

$$\Phi_{\rm halo} = -GM_{\rm halo}\ln(1 + R/R_{\rm halo}), \quad (59)$$

where R, ϖ, and z are the total distance, in the disk radius, and distance above the disk; $R_{\rm bulge}$ (=0.6 kpc), a (=5 kpc), b (=0.3 kpc), and $R_{\rm halo}$ (=20 kpc) are the scaling length for the bulge, disk, and halo, respectively; $M_{\rm SMBH}$ ($=4 \times 10^6 M_\odot$) is the mass of the SMBH; $M_{\rm bulge}$ ($=10^{10}\,M_\odot$), $M_{\rm disk}$ ($=4 \times 10^{10}M_\odot$), and $M_{\rm halo}$ ($=10^{12}M_\odot$) are the mass scaling factor for the bulge, disk, and halo, respectively (Miyamoto & Nagai 1975; Hernquist 1990; Navarro et al. 1997; Dehnen & Binney 1998; Yu & Madau 2007). Various values of these model parameters are summarized in Kenyon et al. (2008).

From the Poisson equation, we find the corresponding density that contributes to these components of the potential:

$$\rho_{\rm bulge} = \frac{M_{\rm bulge}}{4\pi R_{\rm bulge}^3}\frac{(R_{\rm bulge}/R - 1)}{(R/R_{\rm bulge} + 1)^3}, \quad (60)$$

$$\rho_{\rm disk} = \frac{M_{\rm disk}}{4\pi[\varpi^2 + (a + \sqrt{b^2 + z^2})^2]^{3/2}}, \quad (61)$$

$$\rho_{\rm halo} = \frac{M_{\rm halo}}{4\pi R^3}\left[\frac{R(2R + R_{\rm halo})}{(R + R_{\rm halo})^2} - \ln\left(1 + \frac{R}{R_{\rm halo}}\right)\right]. \quad (62)$$

$$\left[\frac{a}{\sqrt{b^2 + z^2}} + \frac{3(a + \sqrt{b^2 + z^2})^2}{\varpi^2 + (a + \sqrt{b^2 + z^2})^2} - \frac{3z^2(1 + a/\sqrt{b^2 + z^2})^2}{\varpi^2 + (a + \sqrt{b^2 + z^2})^2}\right],$$

Deep in the galactic potential where R, ϖ, and z are relatively small compared with other scaling parameters, $\rho_{\rm bulge} \propto R^{-1}$, $\rho_{\rm disk} \sim$ constant, and $\rho_{\rm HALO} \propto R^{-2}$. Only the density associated with the disk potential becomes a slowly varying function of R and z with $k \ll 1$, $\gamma \ll \Omega$, and compressive tidal perturbation. This contribution is negligible over most regions of the Galaxy including the proximity of Sgr A*. In most regions of the present-day Galaxy, the dominant tidal perturbation from other components (SMBH, bulge, and halo) is disruptive. Nevertheless, during the galactic infancy, after the formation of the disk and prior to the formation of a substantial bulge or central black hole, it is possible for stellar clusters to retain their integrity on their migratory routes to the galactic center.

4.4. An Estimate of Inspiral Timescale in the Case of Galactic Centers with Shallow Density Profiles

Nuclear clusters arrive in the galactic center under the action of dynamical friction. In this subsection, we estimate the clusters' typical inspiral timescale $T_{\rm DF}$. For the galactic background potential, we use a general power-law density distribution (37), which, as follows from the previous section, can be used to describe many expected density profiles in inner parts of galaxies. To find $T_{\rm DF}$ we use the expression (8.9) in Binney & Tremaine (2008) to determine the absolute value of force appearing due to the effect of dynamical friction, $\tilde{F}$. Whereas the original calculation is appropriate for the case of $k = 2$, we modify $\tilde{F}$ for a generalized power-law density distribution such that

$$\tilde{F} \approx 5.38\ln\Lambda\frac{G^2M^2\rho_G}{V^2}, \quad (63)$$

where, to be consistent with the notation in other sections, M is the cluster mass, $\ln\Lambda$ is the column logarithm, and $V = \Omega R$ is the cluster's orbital velocity. Note that the orbit is assumed to be nearly circular during the whole orbital evolution. This assumption may not actually be valid for the shallow density profiles, since in this case the orbital eccentricity may grow (Polnarev & Rees 1994; Vecchio et al. 1994). However, we neglect this effect here assuming that it would not significantly change our order-of-magnitude estimates.

In the above expressions, the representative density for the cluster (ρ) is formally less than that of the galactic background (ρ_G) at location $R < R_0$ (where they are equal). However, the total stellar density within the volume occupied by the clusters' stars is the sum of bound cluster stars and that of the galactic stars that merely pass through the cluster. Physically, ρ represents an *overdensity*, and accordingly, mass M is the mass excess.

In order to estimate the dynamical friction timescale,

$$T_{\rm DF} \sim \frac{MV}{\tilde{F}}, \tag{64}$$

we need to specify the mass and spatial scales for both the cluster and its host galaxy. For galaxies with density profile (37), we scale ρ_0 in terms of a reference mass M_G at a given radius R_*. For galaxies similar to the Milky Way (Kenyon et al. 2008), we scale M_G and R_* by dimensionless parameters $M_9 = M_G/10^9\,M_\odot$ and $R_2 = R_*/10^2$ pc. Typical values of M_9 and R_2 are of the order unity. We also scale the cluster's mass M and radius r_0 by dimensionless parameters $m_5 = M/10^5\,M_\odot$ and $r_1 = r_0/10$ pc, respectively. In the scaling in physical units, r_0 corresponds to the half-mass–radius of realistic clusters. Using the above notations, the density profile (37) can be represented as

$$\rho_G(R) = 10^3 \frac{(3-k)}{4\pi}\left(\frac{M_9}{R_2^3}\right)\left(\frac{R}{R_*}\right)^{-k}\frac{M_\odot}{\rm pc^3}, \tag{65}$$

and the typical internal dynamical timescale associated with the cluster

$$\omega_0^{-1} = \sqrt{\frac{R_0^3}{GM}} \approx 1.4\times 10^6\left(\frac{r_1^3}{m_5}\right)^{1/2}\ {\rm yr}. \tag{66}$$

We substitute (63) and (65) in (64) and take into account (38) to obtain

$$T_{\rm DF}(R) \approx \frac{1.75\times 10^8}{\Lambda_{20}}\frac{3M_9}{(3-k)m_5}\left(\frac{R_2^3}{M_9}\right)^{1/2}\left(\frac{R}{R_*}\right)^{3-k/2}\ {\rm yr}, \tag{67}$$

where we assume that a typical value of Λ is of the order of $\ln(10^9) \sim 20$ and $\Lambda_{20} = \Lambda/20$. Equation (67) tells us that the dynamical friction time is reasonably fast for the considered values of numerical parameters, but it sharply grows with R.

It is of interest to compare our tidal disruption radius R_T given by (39) with R_*. Since the condition $\rho_G(R) = \rho_0$ defines the characteristic radius R_0, we find

$$R_0 = \left[10\left(\frac{3-k}{3}\right)\left(\frac{M_9}{m_5}\right)\left(\frac{r_1^3}{R_2^3}\right)\right]^{\frac{1}{k}} R_*. \tag{68}$$

Substituting (68) in (39), we have

$$R_T = \left[10k^4\left(\frac{M_9}{m_5}\right)\left(\frac{r_1^3}{R_2^3}\right)\right]^{\frac{1}{k}} R_*. \tag{69}$$

Thus, the condition $R_T < R_*$ results in

$$k < 0.1^{\frac{1}{4}}\left(\frac{m_5R_2^3}{M_9r_1^3}\right)^{\frac{1}{4}} \approx 0.56\left(\frac{m_5R_2^3}{M_9r_1^3}\right)^{\frac{1}{4}}. \tag{70}$$

This condition rather weakly depends on the ratio of typical densities of the cluster and galaxy. For the considered model parameters, it is typically satisfied. For example, if we adopt the nominal values of these scales with $k = 0.5$, we would find $R_T \approx 0.4R_* \approx 40$ pc.

5. Summary and Discussions

It has long been assumed that tidal perturbation on satellites (including individual stars or stellar clusters) by an external gravitational field is disruptive. However, the conventional tidal disruption radius is derived for a point-mass background potential. This approximation may not be appropriate for a general mass distribution.

In this paper, we examine the tidal stability of stellar clusters in a background gravitational potential with a power-law density distribution. In order to gain some physical insight, we construct an analytic formalism with some idealized assumptions. We consider a cluster with a homogeneous internal density and a circular orbit around an spherically symmetric slowly varying background galactic potential. This approximation is analogous to the classical theory of uniform ellipsoidal figures under tidal perturbation of a companion (Chandrasekhar 1969). The advantage of this approach is that it enabled us to analytically obtain the shape of the cluster and the stellar orbits inside it. We also use these analytic solutions to identify adiabatic invariants that can be used to extrapolate the cluster's adiabatic response from negligible to strong tidal fields through slow (compared with the cluster's internal dynamical timescale) evolution. A similar approach has been used by Young (1980) in his consideration of the adiabatic black hole growth; a similar problem was also recently considered in Jingade et al. (2016) for Sérsic models of elliptical galaxies.

With this method, we calculate the condition under which the stellar orbits become unstable. We show that if the galactic density distribution is a weakly decreasing power-law function of radius, the cluster can preserve its integrity at radii much smaller than the conventional tidal radius, i.e., the cluster can survive deep in the gravitational potential of the galaxy. Although the density inside the survivable clusters is comparable to that of the galactic background, we suggest their accumulation can lead to the gradual buildup of the nuclear clusters.

There are several potential observational tests. The effect of tidal compression enables the clusters to retain their internal velocity dispersion as they undergo orbital decay toward the center of their host galaxies. (1) The nuclear clusters formed along this channel are likely to preserve their velocity dispersion and it is generally smaller than that of the surrounding field stars. (2) When multiple clusters reach the galactic nuclei, the peak of their composite surface density may be slightly displaced from the galactic center. Both of these two dynamical effects have already been suggested and shown through some preliminary simulations by Oh & Lin (2000). (3) If the progenitors of the nuclear clusters originated from the galactic halo with subsolar heavy element abundance, similar to that of the Galactic globular clusters, their convergence at the

galactic centers would enhance the nuclear clusters' metallicity dispersion in contrast to that of the surrounding field stars. However, old and metal-deficient stars transported by the preserved stellar clusters may be outshone by the recently formed young and metal-rich stars, especially in AGNs (Artymowicz et al. 1993).

Our results also show that if background density falls off faster than r^{-1}, the classical tidal radius may still apply. This disruptive effect would occur if the tidal field is dominated by the point-mass potential of SMBHs or possibly by that of galactic bulges. We speculate this dichotomy may be the cause of (1) mutual exclusion between nuclear clusters and SMBHs in the center of massive elliptical galaxies and (2) the dominance of nuclear clusters over black holes in galaxies where they coexist, as in the case of the Milky Way.

Our analytic approach is particularly useful to highlight the basic physical effects. Nevertheless, it is based on idealized models of stellar clusters and adiabatic extrapolation. These models may suffer from many potential instabilities. It is not clear[4] whether these instabilities are physically generic or reflect the very simplified nature of our approach. Although it is technically challenging to extend the analytic analysis to more realistic models with a similar approach, there is a simple argument that enables us to postulate that such models may behave qualitatively in a similar way. Namely, when $\tilde{\gamma}$ is small and the cluster is deep within the potential well of a galaxy so that $\Omega \gg 1$, the cluster's dynamics should be determined by only this frequency. In particular, an orbital period of a "typical" star should be of the order of Ω^{-1}, and accordingly, its energy (per unit of mass) and the corresponding "typical" action should be $E \sim a^2\Omega^2$ and $I \sim a^2\Omega$, respectively, where a is a characteristic size of the cluster. Since the action is conserved we have $a \sim \Omega^{-1/2}$. Now, from Equation (1) it follows that the condition that the combination of tidal and centrifugal forces in the x direction exceeds self-gravity force can be approximately formulated as $\tilde{\gamma}^2\Omega^2 > \frac{Gm}{a^3}$, where we temporarily restore the physical units. Going back to the natural units and substituting $a = \Omega^{-1/2}$ in the condition we have again our tidal disruption criterion (36). Note that, perhaps, this argument can be obtained in a more rigorous way using the formalism based on the virial relations; see, e.g., Osipkov (2006) for the formulation of the problem on hand.

The analytic results presented here verify, in an idealized limit, those of some preliminary numerical simulations by Oh et al. (2000). Those simulations were carried out for several clusters with a more centrally concentrated density distribution (i.e., a King model with $C = 1.8$) embedded in one set of background potential (a King potential with $C = 0.5$ for a dwarf galaxy). Follow-up numerical simulations are needed to verify that centrally concentrated clusters are more tightly bound by their self-gravity and are more resilient to external tidal perturbation. Although such simulations have been carried for a galactic halo potential (Oh & Lin 1992; Oh et al. 1992, 1995), follow-up investigations will be useful to explore the effects of tidal compression for centrally condensed clusters subjected to orbit decay due to dynamical friction in a more general galactic potential. These investigations will be reported elsewhere.

[4] For the similar Freeman bar models such instabilities were considered in Morozov et al. (1974) and Tremaine (1976c).

The authors thank Gordon Ogilvie and John Papaloizou for support and hospitality during the starting point of this project. We also thank the Department of Applied Mathematics and Theoretical Physics, Cambridge University and the Institute for Advanced Studies Tsinghua University for support. We also thank Avishai Dekel, Andrei Doroshkevich, Marla Geha, Puragra Guhathakurta, Anatoly Neishtadt, John Papaloizou, Evgeny Polyachenko, Alexei Rastorguev, Alexander Polnarev, Ilya Shukhman, and Scott Tremaine for useful discussions and comments.

ORCID iDs

D. N. C. Lin https://orcid.org/0000-0001-5466-4628

References

Artymowicz, P., Lin, D. N. C., & Wampler, E. J. 1993, ApJ, 409, 592
Bertin, G., & Varri, A. L. 2008, ApJ, 689, 1005
Binggeli, B., & Cameron, L. M. 1991, A&A, 252, 27
Binney, J., & Tremaine, S. 2008, Galactic Dynamics: Second Edition (Princeton, NJ: Princeton Univ. Press)
Blumenthal, G. R., Faber, S. M., Primack, J. R., & Rees, M. J. 1984, Natur, 311, 517
Böker, T., Laine, S., van der Marel, R. P., et al. 2002, AJ, 123, 1389
Capuzzo-Dolcetta, R. 1993, ApJ, 415, 616
Chandrasekhar, S. 1969, Ellipsoidal Figures of Equilibrium (New Haven, CT: Yale Univ. Press)
Côté, P., Piatek, S., Ferrarese, L., et al. 2006, ApJS, 165, 57
Cotera, A. S., Erickson, E. F., Colgan, S. W. J., et al. 1996, ApJ, 461, 750
Davis, M., Efstathiou, G., Frenk, C. S., & White, S. D. M. 1985, ApJ, 292, 371
Deason, A. J., Belokurov, V., Koposov, S. E., & Lancaster, L. 2018, ApJL, 862, L1
Dehnen, W., & Binney, J. 1998, MNRAS, 294, 429
Dekel, A., Arad, I., Devor, J., & Birnboim, Y. 2003a, ApJ, 588, 680
Dekel, A., Devor, J., & Hetzroni, G. 2003b, MNRAS, 341, 326
Do, T., Ghez, A. M., Morris, M. R., et al. 2009, ApJ, 703, 1323
Drinkwater, M. J., Gregg, M. D., Hilker, M., et al. 2003, Natur, 423, 519
Emsellem, E., & van de Ven, G. 2008, ApJ, 674, 653
Espinoza, P., Selman, F. J., & Melnick, J. 2009, A&A, 501, 563
Fall, S. M., & Rees, M. J. 1977, MNRAS, 181, 37P
Fellhauer, M., & Lin, D. N. C. 2007, MNRAS, 375, 604
Ferguson, H. C., & Sandage, A. 1991, AJ, 101, 765
Ferrarese, L., Côté, P., Dalla Bontà, E., et al. 2006, ApJL, 644, L21
Ferrarese, L., & Ford, H. 2005, SSRv, 116, 523
Ferrarese, L., & Merritt, D. 2000, ApJL, 539, L9
Figer, D. F., McLean, I. S., & Morris, M. 1999, ApJ, 514, 202
Figer, D. F., & Morris, M. 2002, in ASP Conf. Ser. 285, Starburst Clusters in Galactic Nuclei (Invited), ed. E. K. Grebel & W. Brandner (San Francisco, CA: ASP), 381
Frank, J., & Rees, M. J. 1976, MNRAS, 176, 633
Freeman, K. C. 1966a, MNRAS, 133, 47
Freeman, K. C. 1966b, MNRAS, 134, 1
Freeman, K. C. 1966c, MNRAS, 134, 15
Gebhardt, K., Bender, R., Bower, G., et al. 2000, ApJL, 539, L13
Genzel, R., Eckart, A., Ott, T., & Eisenhauer, F. 1997, MNRAS, 291, 219
Genzel, R., Eisenhauer, F., & Gillessen, S. 2010, RvMP, 82, 3121
Gerhard, O. 2001, ApJL, 546, L39
Ghez, A. M., Duchêne, G., Matthews, K., et al. 2003, ApJL, 586, L127
Ghez, A. M., Klein, B. L., Morris, M., & Becklin, E. E. 1998, ApJ, 509, 678
Gilbert, K. M., Font, A. S., Johnston, K. V., & Guhathakurta, P. 2009, ApJ, 701, 776
Gnedin, O. Y., Gould, A., Miralda-Escudé, J., & Zentner, A. R. 2005, ApJ, 634, 344
Goerdt, T., Moore, B., Kazantzidis, S., et al. 2008, MNRAS, 385, 2136
Goodman, J. 2003, MNRAS, 339, 937
Graham, A. W., & Driver, S. P. 2005, PASA, 22, 118
Guhathakurta, P., Rich, R. M., Reitzel, D. B., et al. 2006, AJ, 131, 2497
Gürkan, M. A., & Rasio, F. A. 2005, ApJ, 628, 236
Helmi, A., Babusiaux, C., Koppelman, H. H., et al. 2018, Natur, 563, 85
Hernandez, X., & Gilmore, G. 1998, MNRAS, 297, 517
Hernquist, L. 1990, ApJ, 356, 359
Ibata, R. A., Gilmore, G., & Irwin, M. J. 1994, Natur, 370, 194

Jaffe, W. 1983, MNRAS, 202, 995
Jingade, N., Deep Saini, T., & Tremaine, S. 2016, AJ, 151, 119
Johnston, K. V., Spergel, D. N., & Hernquist, L. 1995, ApJ, 451, 598
Just, A., Khan, F. M., Berczik, P., Ernst, A., & Spurzem, R. 2011, MNRAS, 411, 653
Kenyon, S. J., Bromley, B. C., Geller, M. J., & Brown, W. R. 2008, ApJ, 680, 312
Kobayashi, Y., Okuda, H., Sato, S., Jugaku, J., & Dyck, H. M. 1983, PASJ, 35, 101
Koppelman, H., Helmi, A., & Veljanoski, J. 2018, ApJL, 860, L11
Kormendy, J., Fisher, D. B., Cornell, M. E., & Bender, R. 2009, ApJS, 182, 216
Kormendy, J., & Ho, L. C. 2013, ARA&A, 51, 511
Levin, Y., & Beloborodov, A. M. 2003, ApJL, 590, L33
Lynden-Bell, D. 1969, Natur, 223, 690
Lynden-Bell, D., & Lynden-Bell, R. M. 1995, MNRAS, 275, 429
Madigan, A.-M., Pfuhl, O., Levin, Y., et al. 2014, in IAU Symp. 303, The Galactic Center: Feeding and Feedback in a Normal Galactic Nucleus, ed. L. O. Sjouwerman, C. C. Lang, & J. Ott (Cambridge: Cambridge Univ. Press), 238
Masi, M. 2007, AmJPh, 75, 116
Miller, B. W., & Lotz, J. M. 2007, ApJ, 670, 1074
Misgeld, I., & Hilker, M. 2011, MNRAS, 414, 3699
Mitchell, D. G. M., & Heggie, D. C. 2007, MNRAS, 376, 705
Miyamoto, M., & Nagai, R. 1975, PASJ, 27, 533
Morozov, A. G., Polyachenko, V. L., & Shukhman, I. G. 1974, SvA, 18, 44
Myeong, G. C., Evans, N. W., Belokurov, V., Amorisco, N. C., & Koposov, S. E. 2018, MNRAS, 475, 1537
Myeong, G. C., Vasiliev, E., Iorio, G., Evans, N. W., & Belokurov, V. 2019, MNRAS, 488, 1235
Nagata, T., Woodward, C. E., Shure, M., & Kobayashi, N. 1995, AJ, 109, 1676
Navarro, J. F., Frenk, C. S., & White, S. D. M. 1995, MNRAS, 275, 56
Navarro, J. F., Frenk, C. S., & White, S. D. M. 1996, ApJ, 462, 563
Navarro, J. F., Frenk, C. S., & White, S. D. M. 1997, ApJ, 490, 493
Nayakshin, S., Cuadra, J., & Springel, V. 2007, MNRAS, 379, 21
Necib, L., Lisanti, M., & Belokurov, V. 2019, ApJ, 874, 3
Neumayer, N., Seth, A., & Böker, T. 2020, A&ARv, 28, 4
Newberg, H. J., & Carlin, J. L. 2016, Tidal Streams in the Local Group and Beyond (Berlin: Springer)
Oh, K. S., & Lin, D. N. C. 1992, ApJ, 386, 519
Oh, K. S., & Lin, D. N. C. 2000, ApJ, 543, 620
Oh, K. S., Lin, D. N. C., & Aarseth, S. J. 1992, ApJ, 386, 506
Oh, K. S., Lin, D. N. C., & Aarseth, S. J. 1995, ApJ, 442, 142
Oh, K. S., Lin, D. N. C., & Richer, H. B. 2000, ApJ, 531, 727
Osipkov, L. P. 2006, ARep, 50, 116
Ostriker, J. P., Spitzer, L. J., & Chevalier, R. A. 1972, ApJL, 176, L51
Pfeffer, J., Griffen, B. F., Baumgardt, H., & Hilker, M. 2014, MNRAS, 444, 3670
Polnarev, A. G., & Rees, M. J. 1994, A&A, 283, 301
Portegies Zwart, S. F., Makino, J., McMillan, S. L. W., & Hut, P. 2002, ApJ, 565, 265
Prugniel, P., & Simien, F. 1997, A&A, 321, 111
Sandage, A., & Binggeli, B. 1984, AJ, 89, 919
Sersic, J. L. 1968, Atlas de Galaxias Australes (Cordoba: Observatorio Astronomico)
Terzić, B., & Graham, A. W. 2005, MNRAS, 362, 197
Tremaine, S., Richstone, D. O., Byun, Y.-I., et al. 1994, AJ, 107, 634
Tremaine, S. D. 1976a, ApJ, 203, 345
Tremaine, S. D. 1976b, ApJ, 203, 72
Tremaine, S. D. 1976c, MNRAS, 175, 557
Tremaine, S. D., Ostriker, J. P., & Spitzer, L. J. 1975, ApJ, 196, 407
Valluri, M. 1993, ApJ, 408, 57
van der Marel, R. P., Rossa, J., Walcher, C. J., et al. 2007, in IAU Symp. 241, Stellar Populations as Building Blocks of Galaxies, ed. A. Vazdekis & R. Peletier (Cambridge: Cambridge Univ. Press), 475
Vecchio, A., Colpi, M., & Polnarev, A. G. 1994, ApJ, 433, 733
Wang, M. Y., Koposov, S., Drlica-Wagner, A., et al. 2019, ApJL, 875, L13
White, S. D. M., & Rees, M. J. 1978, MNRAS, 183, 341
Widrow, L. M., & Dubinski, J. 2005, ApJ, 631, 838
Young, P. 1980, ApJ, 242, 1232
Yu, Q., & Madau, P. 2007, MNRAS, 379, 1293